AJNR

Early Postnatal Development of Corpus Callosum and Corticospinal White Matter Assessed with Quantitative Tractography

J.H. Gilmore, W. Lin, I. Corouge, Y.S.K. Vetsa, J.K. Smith, C. Kang, H. Gu, R.M. Hamer, J.A. Lieberman and G. Gerig

AJNR Am J Neuroradiol 2007, 28 (9) 1789-1795
doi: https://doi.org/10.3174/ajnr.A0751
http://www.ajnr.org/content/28/9/1789

ORIGINAL RESEARCH

Early Postnatal Development of Corpus Callosum and Corticospinal White Matter Assessed with Quantitative Tractography

J.H. Gilmore
W. Lin
I. Corouge
Y.S.K. Vetsa
J.K. Smith
C. Kang
H. Gu
R.M. Hamer
J.A. Lieberman
G. Gerig

BACKGROUND AND PURPOSE: The early postnatal period is perhaps the most dynamic phase of white matter development. We hypothesized that the early postnatal development of the corpus callosum and corticospinal tracts could be studied in unsedated healthy neonates by using novel approaches to diffusion tensor imaging (DTI) and quantitative tractography.

MATERIALS AND METHODS: Isotropic $2 \times 2 \times 2$ mm^3 DTI and structural images were acquired from 47 healthy neonates. DTI and structural images were coregistered and fractional anisotropy (FA), mean diffusivity (MD), and normalized T1-weighted (T1W) and T2-weighted (T2W) signal intensities were determined in central midline and peripheral cortical regions of the white matter tracts of the genu and splenium of the corpus callosum and the central midbrain and peripheral cortical regions of the corticospinal tracts by using quantitative tractography.

RESULTS: We observed that central regions exhibited lower MD, higher FA values, higher T1W intensity, and lower T2W intensity than peripheral cortical regions. As expected, MD decreased, FA increased, and T2W signal intensity decreased with increasing age in the genu and corticospinal tract, whereas there was no significant change in T1W signal intensity. The central midline region of the splenium fiber tract has a unique pattern, with no change in MD, FA, or T2W signal intensity with age, suggesting different growth trajectory compared with the other tracts. FA seems to be more dependent on tract organization, whereas MD seems to be more sensitive to myelination.

CONCLUSIONS: Our novel approach may detect small regional differences and age-related changes in the corpus callosum and corticospinal white matter tracts in unsedated healthy neonates and may be used for future studies of pediatric brain disorders that affect developing white matter.

The early postnatal period is perhaps the most dynamic phase of brain development. Cortical gray matter volumes increase significantly in the first weeks after birth,[1] consistent with synapse development.[2] Myelination of white matter also proceeds rapidly.[3] Concurrent with structural brain development is an equally rapid development of a wide range of cognitive and motor functions,[4] and it has been proposed that myelination parallels functional maturation.[5] Postmortem studies indicate myelination occurs in proximal pathways before distal pathways, in central sites before poles, and in the occipital poles before the frontotemporal poles.[3,6]

The myelination status of white matter on MR imaging is determined by the relative intensity of T1-weighted (T1W) and T2-weighted (T2W) signals.[3,7] The relationship of the composition and the microscopic structure of brain tissue and its T1 and T2 signal intensity is very complex and not well understood, especially in the context of the developing brain.[3,7] Diffusion tensor imaging (DTI) has provided a new approach to understanding the development of white matter tracts. Results from studies in premature infants using region-of-interest approaches indicate that mean diffusivity (MD) in central white matter tracts decreases with age, whereas fractional anisotropy (FA) increases.[8-10] Studies of older children show rapid maturation of MD and FA values in the corpus callosum and internal capsule over the first 2 years of life.[11-14] In normal neonates, we observed a lag in peripheral cortical white matter maturation compared with central white matter tracts.[15,16] A recent study reported generally rapid changes of FA and fiber tract size in the first 12 months, with relative stability after 24 months.[17]

Most DTI studies in children have been limited to 2D region-of-interest approaches that do not capture the complexity of 3D white matter tracts. The feasibility of quantitative tractography has been demonstrated in premature infants[18,19] and in infants with perinatal hypoxic ischemia.[20] We hypothesized that the early postnatal development of the corpus callosum and corticospinal tracts could be studied in unsedated healthy neonates with DTI and quantitative tractography. We used a 3T scanner (which provides improved DTI tractography compared with 1.5T[21]), a novel quantitative analysis of complex regions of interest,[22,23] along with coregistration of DTI images with structural T1W and T2W images to study the development of diffusion properties in the corpus callosum and the corticospinal tracts and their relationship to T1W and T2W intensities.

Received January 12, 2007; accepted with revisions February 27.

From the Schizophrenia Research Center and Department of Psychiatry (J.H.G., C.K., H.G., R.M.H., G.G.) and the Departments of Radiology (W.L., J.K.S.), Computer Science (I.C., Y.S.K.V., G.G.), and Biostatistics (C.K., H.G., R.M.H.), University of North Carolina, Chapel Hill, NC; and Department of Psychiatry (J.A.L.), Columbia University, New York, NY.

This research was supported by National Institute of Mental Health Silvio Conte Center for Neuroscience of Mental Disorders grant P50-MH064065, National Institutes of Health National Institute of Biomedical Imaging and Bioengineering grant P01-EB002779, and the National Alliance for Medical Image Computing (NAMIC), funded by the National Institutes of Health through the National Institutes of Health Roadmap for Medical Research, grant U54-EB005149.

Previously presented in part at Annual Meeting of the American College of Neuropsychopharmacology, December 5, 2006; Hollywood, Fla.

Please address correspondence to John H. Gilmore, MD, Department of Psychiatry, CB# 7160, University of North Carolina at Chapel Hill, Chapel Hill, NC 27599-7160; e-mail: jgilmore@med.unc.edu

indicates article with supplemental on-line figures

DOI 10.3174/ajnr.A0751

Materials and Methods

Subjects

This study was approved by the Institutional Review Board of the University of North Carolina (UNC) School of Medicine. Infants scanned for this study were healthy control subjects for a larger study of prenatal and neonatal brain development in children at high risk for neurodevelopmental disorders. Control mothers were recruited during the second trimester of pregnancy from the outpatient Obstetrics and Gynecology Clinics at UNC Hospitals. Exclusion criteria were the presence of abnormalities on fetal sonography or major medical or psychotic illness in the mother. Singleton subjects with a gestational age at birth of 37 weeks or older who had both T1W, T2W/proton density, and DTI scans that were free of major motion artifacts were included in this analysis ($n = 49$). Additional exclusion criteria for this analysis included major delivery or neonatal complications or significant central nervous system (CNS) abnormality on MR imaging ($n = 2$). Fourteen subjects had small incidental subdural hematomas or other bleeds, which are present in approximately 25% of vaginal births[24]; these subjects were included in the analysis.

The final study sample ($n = 47$) included 28 boys and 19 girls; ethnic composition was 39 white and 8 African American. There were no significant sex differences in the gestational age at birth (mean ± SD: boys, 39.8 ± 0.9 weeks; girls, 39.5 ± 1.1 weeks; $P = .3230$) or gestational age at MR imaging (boys, 43.1 ± 1.7 weeks; girls, 42.6 ± 1.6 weeks; $P = .3146$). However, there was a significant difference in birth weight between boys and girls (3653.1 ± 450.6 g vs 3146.2 ± 243.6 g, respectively; $P < .0001$).

Image Acquisition

Neonates were scanned unsedated, swaddled, fitted with ear protection, and with their heads secured in a vacuum-fixation device. T1W structural pulse sequences were either a 3D magnetization-prepared rapid acquisition of gradient echo ([MP-RAGE] TR/TI/TE/flip angle, 1820 ms/400 ms/4.38 ms/7°, respectively) or a 3D spoiled gradient (fast low-angle shot [FLASH], TR/TE/flip angle, 15 ms/7 ms/25°, respectively). Proton attenuation and T2W images were obtained with a turbo spin-echo sequence (TSE; TR/TE1/TE2/flip angle, 6200 ms/20 ms/119 ms/150° respectively). Spatial resolution was $1 \times 1 \times 1\text{-mm}^3$ voxel for T1-weighted images, and $1.25 \times 1.25 \times 1.5\text{-mm}^3$ voxel with 0.5-mm intersection gap for proton attenuation/T2-weighted images.

A single-shot echo-planar spin-echo DTI imaging sequence was used with the following parameters: TR, 5200 ms; TE, 73 ms; thickness, 2 mm; in-plane resolution, 2×2 mm^2, and 45 sections. Seven images were acquired for each section, one without diffusion gradient ($b = 0$), and the remaining 6 with $b = 1000\text{s/mm}^2$ and diffusion gradients along $\{1/\sqrt{2}, 0, 1/\sqrt{2}\}$, $\{-1/\sqrt{2}, 0, 1/\sqrt{2}\}$, $\{0, 1/\sqrt{2}, 1/\sqrt{2}\}$, $\{0, 1/\sqrt{2}, -1/\sqrt{2}\}$, $\{1/\sqrt{2}, 1/\sqrt{2}, 0\}$, and $\{-1/\sqrt{2}, 1/\sqrt{2}, 0\}$, separately. To improve signal-to-noise ratio for the DTI images, 5 separate sets of images with 2 averages in each set were acquired. This approach shortens data acquisition time (1.18 min/set) and minimizes motion artifacts.

Preprocessing of Diffusion Tensor Images

Motion can be a challenge when imaging unsedated neonates; averaging DTI scans on the scanner provides insufficient quality for quantitative tractography. To address this issue, each individual directional gradient image was screened off-line for motion artifacts using a novel automatic DTI quality control tool, DTIchecker (http://www.ia.unc.edu/dev). The tool reads the entire DTI dataset, subdivides the images into volumetric stacks of individual gradient directions and repeated acquisitions, and checks the image sections in each volume for artifacts and errors, including intensity artifacts, missing and corrupted sections, and motion artifacts between repeated acquisitions. Images reported as problematic were visualized and compared with neighboring sections and to repeated images in the same gradient directions. Translational and rotational errors were corrected within limits specified by the user, typically 2–3 voxels for translation and 2° maximum for rotation before voxel-by-voxel averaging the repeated acquisitions.

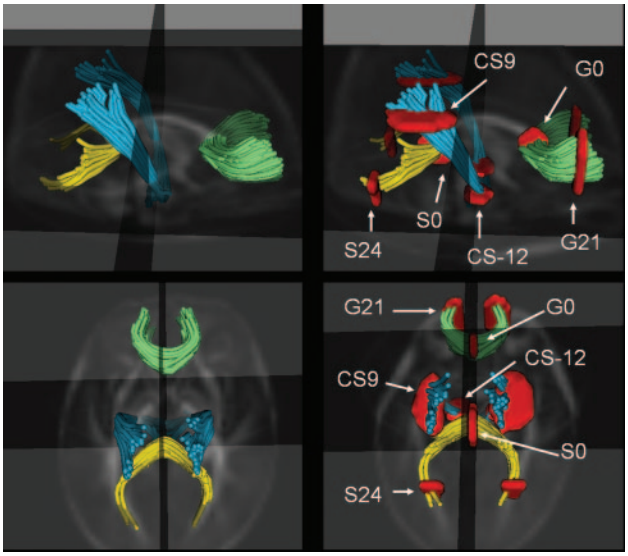

Fig 1. Visualization of the 4 fiber tracts in axial and sagittal views, with overlay of location selected for statistical analysis. Genu (*green*), splenium (*yellow*), and left and right motor tracts (*cyan*) are shown in a 3D display combined with the DTI FA image. CS-12, central corticospinal tract; CS9, cortical corticospinal tract; G0, central genu; G21, cortical genu; S0, central splenium; S24, cortical splenium.

Image Analysis

Quantitative Analysis of Fiber Tracts. We developed a new set of tools for computation of FA and MD maps, tractography (following a concept developed by Mori et al[25] and Xu et al[26]), fiber clustering, and parametrization.[22,23,27,28] Tracts are initialized by drawing source and target regions of interest on FA images. The fiber tracking tool[22,23,29] (http://www.ia.unc.edu/dev) reads the set of diffusion image channels, calculates the tensor field, reads the region-of-interest image, and performs the tracking. The resulting sets of streamlines are stored as lists of polylines that also carry the full tensor information at each location. The method has been tested on splenium and genu tracts in a preliminary feasibility neonate DTI study[27] and was validated in repeated DTI scans of healthy adult volunteers.[30]

For this study, the cross-sectional regions of interest were defined as follows (Fig 1): for the genu and splenium of the corpus callosum, the seed points were the anteriormost and posteriormost aspects of the corpus callosum in the midsagittal plane of the FA image, and one sagittal section on either side. Central regions of the genu (G0) and splenium (S0) were defined as the midsagittal plane; cortical regions were defined as distances from midsagittal plane on the left and right aspects of the fiber tracts: 21 mm from the midsagittal plane for the genu (G21 and G−21), and 24 mm from the midsagittal plane for the splenium (S24 and S−24). For the corticospinal tract, the seed region was defined on the FA image by selecting a region containing the posterior limb of the internal capsule 3 consecutive axial sections. After the tracking, the subgroup/cluster of interest leading to the motor cortex was manually separated. The plane for the fiber plots (or-

thogonal to the fibers, defining the origin) was placed at the top of the corpus callosum in the midsagittal plane; CS9 and CS-12 regions were 9 and 12 mm above and below this plane, respectively. Distances from the central planes to the cortical regions of interest in each tract were chosen so that they had a similar distance from the cortical surface. CS-12 was chosen to capture a region with early myelination.

Reliability. Reliability of the semiautomatic, tractography-based method was tested and compared with manual technique by measures of intraclass correlation (ICC). Five typical image datasets were selected, replicated 3 times, and analyzed in a randomized order. Three trained raters used the quantitative tractography method described above and a manual technique (ITK-SNAP tool[31]) to select regions of interest and to calculate mean FA values per region. Using a mixed model with random effects for image and raters, the ICC's calculated the proportion (in percent) of the total variability in FA measures that can be explained by the variability between the image sets and regions of interest (ROIs) within the same rater (intrarater reliability) or across different raters (inter-rater reliability).[32]

The tractography-based approach produced high-resolution FA measures along tracts (in millimeters from a coordinate origin) at both central and peripheral regions along fibers. The intrarater and inter-rater reliability among the central fiber regions was 0.93 and 0.76, respectively, for the tractography-based approach, similar to 0.95 and 0.77, respectively, for the manual approach. However, manual region drawing failed to determine the off-center peripheral region locations for splenium and genu because the shape and geometry of individual tracts were not discernible on FA images. The intrarater and inter-rater reliability for the tractography-based approach was 0.93 and 0.72, respectively, among these regions.

Combined Analysis of Fiber Tracts Properties in DTI and Structural MRI

Image Calibration. T1W scans were normalized by using T1W values for fatty tissue between the skull and the skin with a 3D level-set segmentation procedure[31] for each subject. Fatty tissue in axial sections of the upper part of the head was seeded, and level-set evolution grew these seeds to capture fatty tissue surrounding the skull. The mean intensity within the resulting thin regions was used as the normalization standard for T1W scans. The differences observed between normalized image data of MPRAGE and FLASH T1 sequences were further corrected by adjusting the group means of FLASH to those of MPRAGE, calculated for each region separately. T2W scans were normalized with T2W values of ventricular CSF. The mean intensity values of these structures were then used as the normalization standard for T2W scans.

Coregistration of DTI and Structural MR Imaging. A nonlinear registration package[33,34] that uses a 3D spline deformation model and mutual information as the image match criterion was used to coregister images. Using a cascaded linear followed by nonlinear deformation, the T2W structural image of each subject was deformed into the baseline image of the DTI scan. Because T1W and T2W structural scans were already coregistered as part of our parallel brain tissue segmentation, the same transformation was applied to map the T1W scan to DTI. Quality control based on a qualitative visual check of overlaid coregistered sets of FA, MD, baseline, T1W, and T2W scans showed that the nonlinear registration step was crucial to bring image modalities sufficiently close for combined analysis. The one-to-one mapping of T1W and T2W images to DTI images allows a straightforward mapping of intensities obtained from T1W and T2W scans to each location represented by the set of fiber tracts. Mean values within cross-sections along the axis of fiber tracts were then calculated for FA, MD, T1W, and T2W parameters and reported for statistical analysis.

Statistical Analysis

For cross-sectional analysis of sex differences of any parameter in any regions, 2-group, 1-way analysis of covariance (ANCOVA) was used, with gestational age at MR imaging used as a covariate. For examinations of asymmetry in each region, we used an ANCOVA on differences to right and left volume differences within subject, with and without controlling age at MR imaging and age from birth to MR imaging as covariates. Analyses were repeated separately for each sex. For comparisons of genu, splenium, and left corticospinal tract in any points, we fit mixed models with region as the within-subject variable of interest without any other covariates. For the developmental trajectory model, we fit mixed models with region as the within-subject variable of interest and age at MR imaging as a continuous predictor. In this model, we examined difference in slope between regions with contrasts. To examine the relationship of T1W and T2W signal intensity to the DTI parameters in each region, we correlated linearly T1W and T2W with each DTI parameter.

Results

For simplicity of description and analysis, we focused on the left cortical and central regions of the corpus callosal fiber tracts passing through the genu and splenium and the central and cortical regions of the left corticospinal tract. There were statistically significant differences only between the right and left cortical region of the genu fiber tract in MD (mean $\pm$ SD; 914.40 $\pm$ 1.47 versus 14.15 $\pm$ 1.66, respectively; $P = .0080$), T1W intensity (44.24 $\pm$ 5.66 versus 43.27 $\pm$ 5.41, respectively; $P < .0001$), and T2W intensity (1216.08 $\pm$ 82.82 versus 1174.20 $\pm$ 88.00, respectively; $P < .0001$); the differences were small in absolute terms. There was no difference between the left and right cortical regions of the splenium or between the left and right central or cortical regions of the corticospinal tracts. There were no sex differences of any parameter in any region (data not shown).

MD was significantly different across all ROIs studied in the genu, splenium, and left corticospinal tract (ANCOVA $P < .0001$; Fig 2). Comparison of individual regions revealed that the MD of the central splenium (S0) was significantly higher than the central region of the genu (G0; $P < .05$). Likewise, the peripheral region of the splenium (S24) had a higher MD than the peripheral region of the genu (G21; $P < .05$). The myelinated central region of the left corticospinal tract (CS-12) had the lowest MD compared with all other regions, including the peripheral region of the corticospinal tract (SC9; $P < .001$ for each comparison).

FA was significantly different across all ROIs studied in the genu, splenium, and left corticospinal tract (ANCOVA $P < .0001$; Fig 3). The central portion had a significantly higher FA than the peripheral region genu ($P < .001$), splenium ($P < .001$), and left corticospinal tract, ($P < .001$). The central portion of the splenium (S0) had significantly higher FA values than the central regions of the genu (G0, $P < .001$) or the myelinated central region of the corticospinal tract (CS-12; $P < .001$). Finally, the FA of the peripheral region of the splenium (S24) was significantly higher than the peripheral region of the genu (G0; $P < .001$).

In the relatively narrow age range of our sample, we were able to detect age-related changes in FA and MD in fibers of

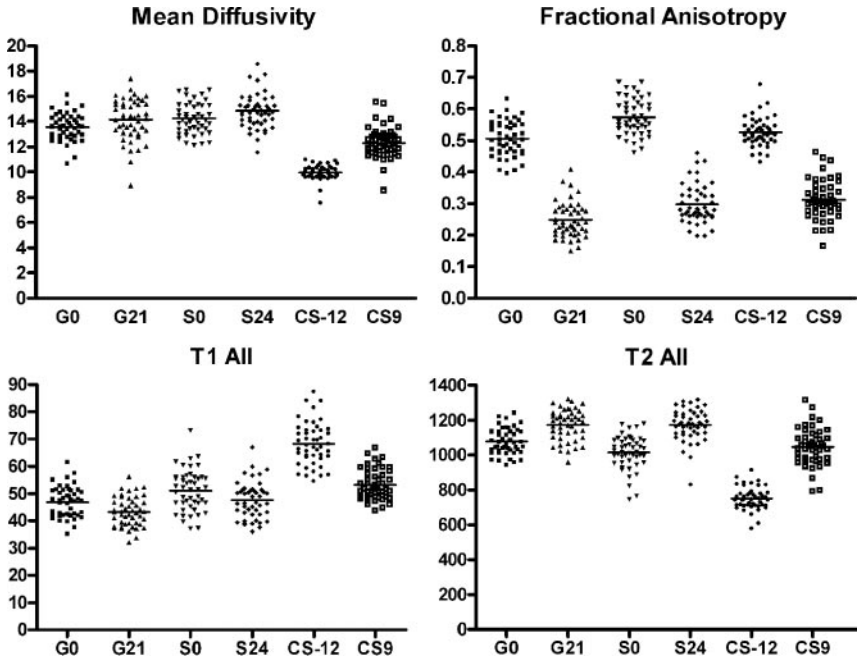

Fig 2. Mean diffusivity, fractional anisotropy, T1w and T2w signal intensity in the major white matter tracts of the neonate ($n = 47$). See "Results" for details of statistical analysis.

the genu and corticospinal tract (Fig 3). In both central and peripheral cortical portions of the genu and the left corticospinal tract, FA increased significantly and MD decreased significantly with increasing age at MR imaging. It is noteworthy that this maturational pattern is not present in the splenium, where FA and MD were not significantly changed with age in either the central or peripheral cortical regions.

T1W signal intensity was significantly different across all white matter tract regions (ANCOVA, $P < .0001$; Fig 4). T1W signal intensity was significantly higher in the central compared with the peripheral regions of the genu ($P < .001$), splenium ($P < .001$), and corticospinal tract ($P < .001$). The central region of the corticospinal tract had a significantly higher T1W signal intensity than all other regions ($P < .001$ for each region).

T2W signal intensity was significantly different across all white matter tract regions (ANCOVA, $P < .0001$; Fig 4). T2W signal intensity was significantly lower in the central compared with the peripheral regions of the genu ($P < .001$), splenium ($P < .001$), and corticospinal tract ($P < .001$). The myelinated central region of the corticospinal tract had significantly lower T2 intensity than all other regions ($P < .001$ for each region).

T1W signal intensity did not change with age in the narrow age range of our cohort in any region (Fig 4). T2 signal intensity significantly declined with age in all regions except the central region of the splenium (Fig 4).

We studied the relationship of T1W and T2W signal intensity to the DTI parameters MD and FA in each white matter tract region. For T1W signal intensity, there was no significant correlation with MD, except in the cortical region of the splenium ($r^2 = 0.1602$; $P = .0053$; Fig 5, supplemental on-line figure). There were no significant correlations of T1 signal intensity with FA in any region ($P > .05$ for each region; Fig 5, supplemental on-line figure). In contrast, T2 signal intensity was positively correlated with MD and negatively correlated with FA in each region (Fig 6, supplemental on-line figure).

Discussion

Our results are consistent with general principles of white matter maturation in the developing brain observed in previous postmortem and imaging studies—central regions of white matter tracts were more mature and organized than peripheral cortical regions, with lower MD and higher FA values. This pattern also was observed with T1W and T2W signal intensity; central regions of each white matter tract had higher T1W intensity and lower T2W intensity than peripheral cortical portions.

Comparison of the splenium and the genu is consistent with the posterior-to-anterior maturation of white matter described in previous studies.[3,6] In both the central and peripheral cortical regions, FA is higher, T1W signal intensity is higher, and T2W signal intensity is lower compared with the genu, reflecting more mature white matter tracts. The exception to this pattern is MD, which is actually higher in both the central and peripheral cortical regions of the splenium compared with the genu.

In the white matter tracts of the genu and corticospinal tract, we detected the expected changes related to increasing age: decreasing MD, increasing FA, and decreasing T2W signal intensity. In the genu and corticospinal tract, there was no significant change in T1W signal intensity with age. Therefore, T2W signal intensity appears to be more sensitive to maturational events in white matter than the T1W signal intensity, at least during the narrow age range of our neonatal cohort. This finding is consistent with a previous study of white matter tract maturation in rodents that reported T2W sequences shortened but T1W sequences did not change, even in the presence of myelination.[35] Our study suggests that T2W signal intensity does decrease significantly in white matter tracts even before myelination is grossly evident on MR imaging.

We were surprised not to observe this maturational pattern in the splenium. There is no change in MD or FA with age in either the central or peripheral cortical regions. In the central region of the splenium, T2W signal intensity did not decrease with age, and T1W signal intensity decreased, a pattern different from that observed in the genu and corticospinal tract. The change in T1W and T2W signal intensity with age in the peripheral cortical region of the splenium was similar to that in other regions. Taken together, these findings suggest that there is a different growth trajectory in the splenium during the neonatal period compared with the genu or corticospinal tract. In the nonhuman primate, myelination occurs more rapidly in the posterior regions of the corpus callosum compared with the anterior regions.[36] Approximately 70% of axons in the corpus callosum also are eliminated in the first 4 months after birth; the posterior region of the corpus callosum has a larger decline in axon attenuation than other regions.[36] We observed that cortical gray matter growth was much faster in the occipital and parietal regions compared with the pre-

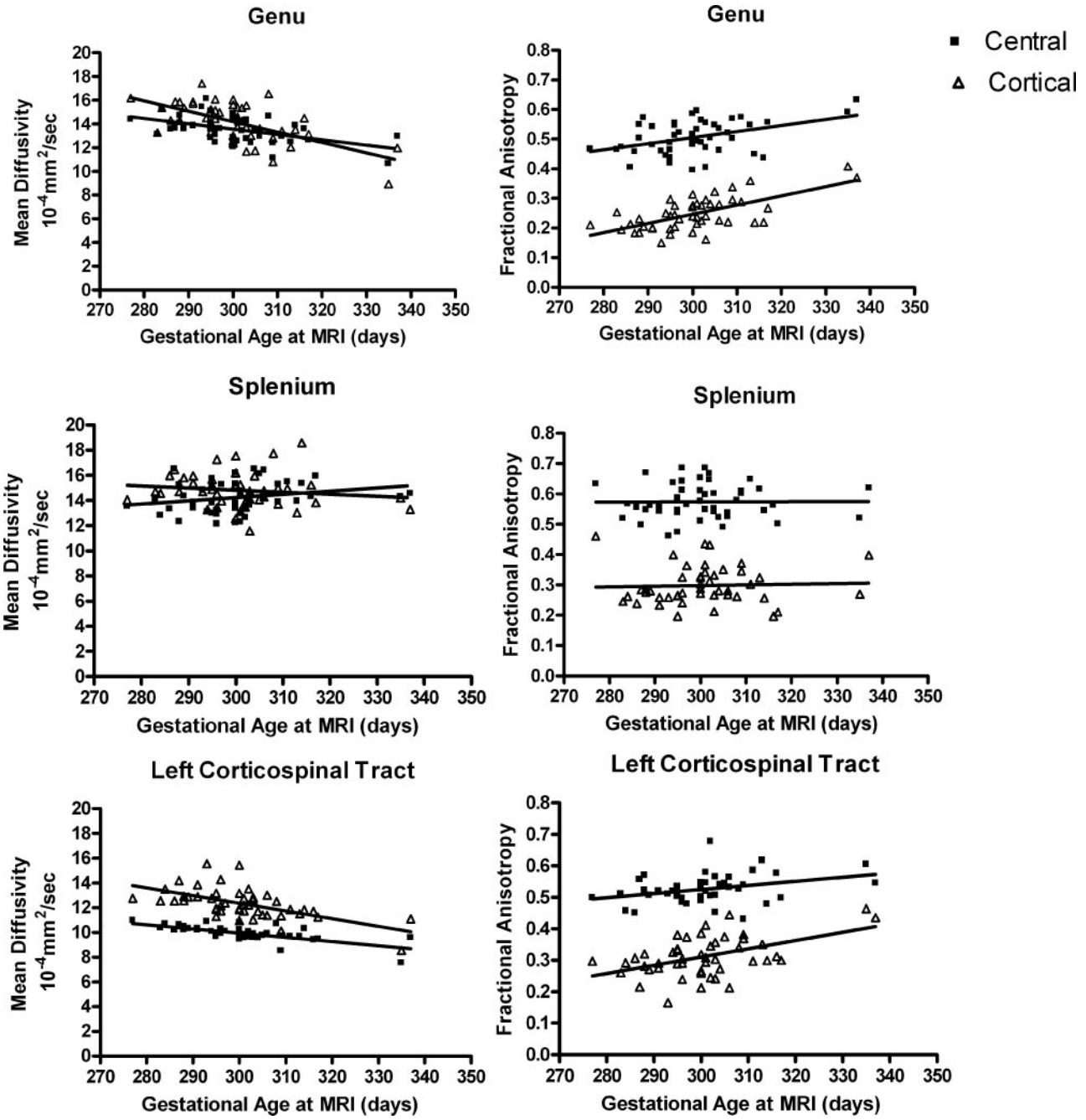

Fig 3. Maturation of mean diffusivity (MD) and fractional anisotropy (FA) in white matter tracts of the genu, splenium, and left corticospinal tract ($n = 47$). In the genu, MD was significantly correlated with age in the central ($r^2 = 0.2392$; $P = .0005$) and peripheral ($r^2 = 0.3781$; $P < .0001$) regions. FA also was significantly correlated with age in the central ($r^2 = 0.1810$; $P = .0029$) and peripheral ($r^2 = 0.4219$; $P < .0001$) regions. Unlike other fiber tracts studied, there were no significant correlations of age with MD in the central ($r^2 = 0.05944$; $P = .0986$) and peripheral ($r^2 = 0.02135$; $P = .3271$) regions of the splenium. In the splenium, FA also was not significantly correlated with age in the central ($r^2 = 0.000027$; $P = .9720$) and peripheral ($r^2 = 0.00175$; $P = .7800$) regions. In the left corticospinal tract, MD was significantly correlated with age in the central ($r^2 = 0.3447$; $P < .0001$) and peripheral ($r^2 = 0.4727$; $P < .0001$) regions. FA was significantly correlated with age in the central ($r^2 = 0.2363$; $P = .0005$) and peripheral ($r^2 = 0.1138$; $P < .0204$) regions.

frontal regions,[1] suggesting a posterior-to-anterior functional maturation of gray matter that also may be evident in the white matter tracts of the corpus callosum.

The relationship between diffusion properties and myelination of white matter tracts is not clear. We observed high degrees of FA that increased with age in the unmyelinated central regions of the genu and splenium; in fact, the FA of the unmyelinated central splenium was significantly higher than the myelinated central region of the corticospinal tract. Anisotropy has been demonstrated in unmyelinated fiber tracts in garfish and lobster, indicting that the structure of fibers can give rise to anisotrophy independent of myelination.[37] Anisotropy also has been observed in white matter tracts of the CNS in rats[35,38] and in premature humans.[8,9] A recent study in rabbits reported that FA increased before and reached a plateau after the onset of myelination, suggesting that immature oligodendrocytes may contribute to structural and functional maturation of white matter fiber tracts before myelination.[39]

The maturation of FA appears to be related more to the organization of the fiber tracts than to the presence of myelin

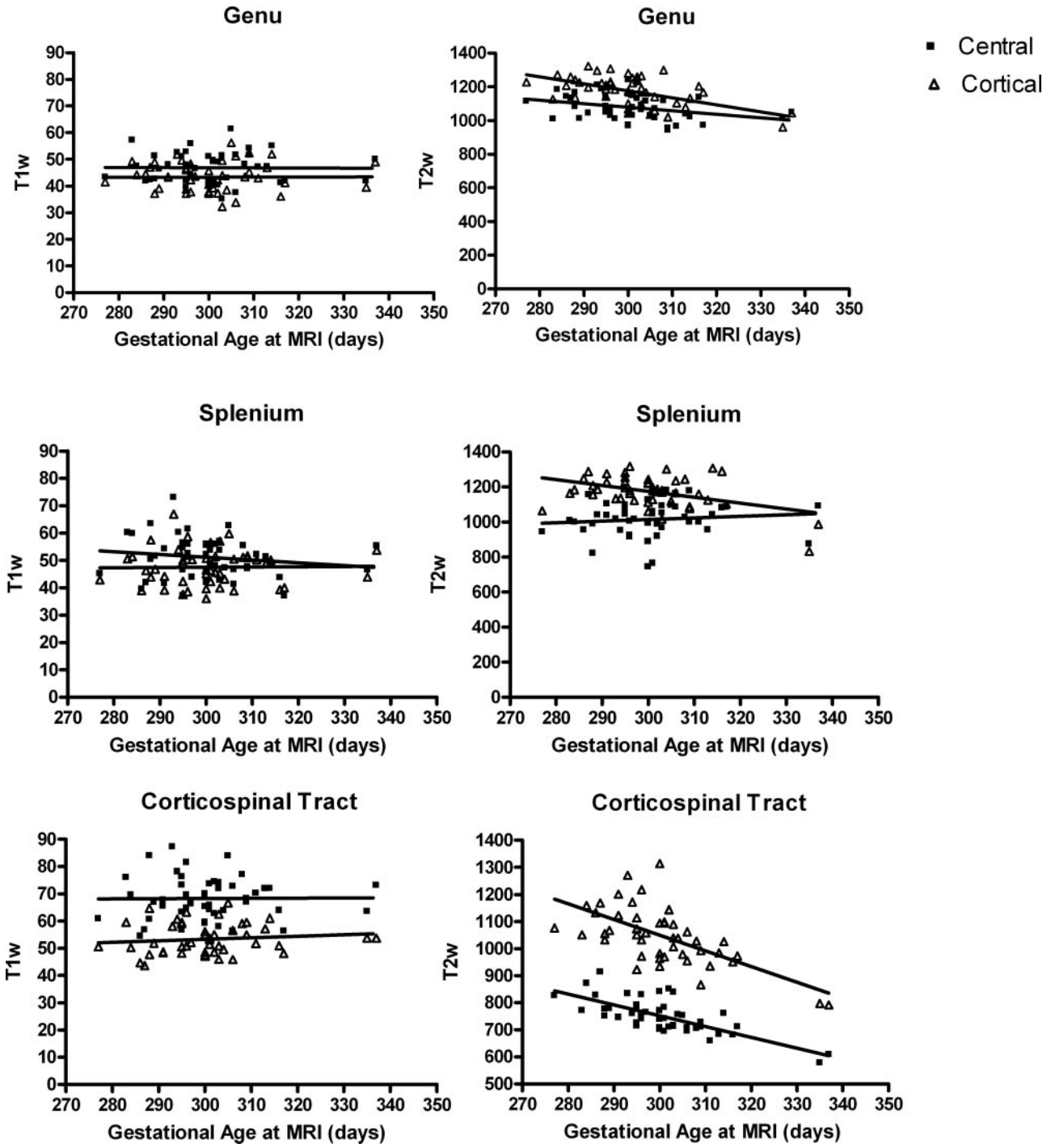

Fig 4. Age-related changes in T1W and T2W signal intensity in the white matter tracts of the genu, splenium, and left corticospinal tract. In the genu, T1W signal intensity was not significantly correlated with age in either the central ($r^2 = 0.03823$; $P = .2461$) or peripheral region ($r^2 = 0.005794$; $P = .6543$). T2W signal intensity significantly declined with age in both the central ($r^2 = 0.09326$; $P = .0348$) and peripheral regions ($r^2 = 0.2891$; $P = .0001$). A similar overall pattern is present in the left corticospinal tract. T1W signal intensity was not significantly correlated with age in either the central ($r^2 = 0.02530$; $P = .3541$) or peripheral region ($r^2 = 0.005692$, $P = .6619$) and T2W signal intensity decreases with age in both the central ($r^2 = 0.5204$, $P < .0001$.) and cortical peripheral ($r^2 = 0.3975$; $P < .0001$) regions. In the splenium, a different pattern is evident. T1W signal intensity decreases with age in the central ($r^2 = 0.1207$; $P = .0352$) but not the peripheral region ($r^2 = 0.01349$; $P = .4937$). T2W signal intensity significantly decreased with age in the peripheral region ($r^2 = 0.1818$; $P = .0025$), but not in the central region ($r^2 = 0.01067$; $P = .4848$).

in the tracts. Conversely, MD appeared to be more sensitive to myelination, with lowest values in the myelinated central region of the corticospinal tract (CS-12). It would seem that water diffusion is highly restricted at CS-12 compared with the central region of the genu (G0) or splenium (S0) of the corpus callosum, though G0 and S0 may have more coherent directionality for the fiber tracts and thus exhibit FA similar to CS-12 with a higher MD.

To some extent, T2W intensity also provides a measure of water diffusion in addition to providing the water content information. Therefore, one would expect that the results shown in the measures of T2W would be similar to that using MD. This is indeed the case in

our study in which similar patterns of T2W intensity and MD are observed in the different regions (Figs 4, 6 [supplemental on-line figure]).

One of the potential confounding factors for the interpretation of our results is the lack of independent measures of brain water content, as regional differences in brain water content may also alter the measures of MD, T1W and T2W, though would have minimal effects on FA values. For example, Fig 2 suggests that the central splenium (S0) has a significantly higher MD compared with the central genu (G0), indicating that brain water diffusion is more restricted in G0 than S0. In contrast, the FA value in S0 is significantly higher than in G0, suggesting that it has a higher anisotropic diffusion than the G0. Together, these findings suggest that although water diffusion is more restricted in G0 than in S0, the water restriction at G0 is more isotropic in nature, whereas anisotropic diffusion is more prominent in S0. Although several plausible physiologic underpinnings can explain these findings, one could speculate that the brain water content may be higher and the biologic barriers less organized at G0 than in S0; as a result, both MD and FA are lower at G0. This potential explanation is further supported by the measures of T1W and T2W signal intensity; S0 has a higher T1W and lower T2W signal intensity than G0. Nevertheless, unless brain water content is measured independently, one must be cautious in interpreting results of MD, T1W, and T2W.

Conclusion

This study demonstrates that development of the corpus callosum and corticospinal tracts can be studied in unsedated healthy neonates by using quantitative tractography of DTI images. Overall, our approach provides very consistent MD and FA values within specific regions of white matter tracts and is able to detect small regional differences and age-related changes in the neonatal period. In general, we found that central regions of white matter tracts were more mature and organized than peripheral cortical regions, with lower MD and higher FA values. White matter tracts of the splenium have a different developmental trajectory than those of the genu, perhaps reflecting differences in functional maturation.

Acknowledgments

We thank Kathy Wilber for technical assistance and Dianne Evans for study coordination.

References

1. Gilmore JH, Lin W, Prastawa MW, et al. **Regional gray matter growth, sexual dimorphism and cerebral asymmetry in the neonatal brain.** *J Neurosci* 2007;27:1255–60
2. Huttenlocher PR, Dabholkar AS. **Regional differences in synaptogenesis in human cerebral cortex.** *J Comp Neurol* 1997;387:167–78
3. Sampaio RC, Truwit CL. **Myelination in the developing brain.** In: Nelson CA, Luciana M, eds. *Handbook of Developmental Cognitive Neuroscience.* Cambridge, Mass: MIT Press; 2001:35–44
4. Kagen J, Herschkowitz N. *A Young Mind in a Growing Brain.* Mahwah, NJ: Lawrence Erlbaum Associates; 2005
5. Yakovlev PI, Lecours AR. **The myelogenetic cycles of regional brain maturation of the brain.** In: Mankowski A, editor. *Regional Development of the Brain in Early Life.* Philadelphia: Davis; 1967:3–69
6. Kinney HC, Brody BA, Kloman AS, et al. **Sequence of central nervous system myelination in human infancy. II. Patterns of myelination in autopsied infants.** *J Neuropathol Exp Neurol* 1988;47:217–34
7. Paus T, Collins DL, Evans AC, et al. **Maturation of white matter in the human brain: a review of magnetic resonance studies.** *Brain Res Bull* 2001;54:255–66
8. Huppi PS, Maier SE, Peled S, et al. **Microstructural development of human newborn cerebral white matter assessed in vivo by diffusion tensor magnetic resonance imaging.** *Pediatr Res* 1998;44:584–90
9. Neil JJ, Shiran SI, McKinstry RC, et al. **Normal brain in human newborns: apparent diffusion coefficient and diffusion anisotropy measured by using diffusion tensor MR imaging.** *Radiology* 1998;209:57–66
10. Partridge SC, Mukherjee P, Berman JI, et al. **Tractography-based quantitation of diffusion tensor imaging parameters in white matter tracts of preterm newborns.** *J Magn Reson Imaging* 2005;22:467–74
11. Mukherjee P, Miller JH, Shimony JS, et al. **Normal brain maturation during childhood: developmental trends characterized with diffusion-tensor MR imaging.** *Radiology* 2001;221:349–58
12. Mukherjee P, Miller JH, Shimony JS, et al. **Diffusion-tensor MR imaging of gray and white matter development during normal human brain maturation.** *AJNR Am J Neuroradiol* 2002;23:1445–56
13. Schmithorst VJ, Wilke M, Dardzinski BJ, et al. **Correlation of white matter diffusivity and anisotropy with age during childhood and adolescence: a cross-sectional diffusion-tensor MR imaging study.** *Radiology* 2002;222:212–18
14. Zhang L, Thomas KM, Davidson MC, et al**. MR quantitation of volume and diffusion changes in the developing brain.** *AJNR Am J Neuroradiol* 2005;26:45–49
15. Gilmore JH, Zhai G, Wilber K, et al. **3 Tesla magnetic resonance imaging of the brain in newborns.** *Psychiatry Res* 2004;132:81–85
16. Zhai G, Lin W, Wilber K, et al. **Comparisons of regional white matter diffusion in healthy neonates and adults using a 3.0-T head-only scanner.** *Radiology* 2003;229:673–81
17. Hermoye L, Saint-Martin C, Cosnard G, et al. **Pediatric diffusion tensor imaging: normal database and observation of the white matter maturation in early childhood.** *Neuroimage* 2006;29:493–504
18. Berman JI, Mukherjee P, Partridge SC, et al. **Quantitative diffusion tensor MRI fiber tractography of sensorimotor white matter development in premature infants.** *Neuroimage* 2005;27:862–71
19. Partridge SC, Mukherjee P, Henry RG, et al. **Diffusion tensor imaging: serial quantitation of white matter tract maturity in premature newborns.** *Neuroimage* 2004;22:1302–14
20. van Pul C, Buijs J, Vilanova A, et al. **Infants with perinatal hypoxic ischemia: feasibility of fiber tracking at birth and 3 months.** *Radiology* 2006;240:203–14
21. Okada T, Miki Y, Fushimi Y, et al. **Diffusion-tensor fiber tractography: intraindividual comparison of 3.0-T and 1.5-T MR imaging.** *Radiology* 2006;238:668–78
22. Corouge I, Fletcher PT, Joshi S, et al. **Fiber tract-oriented statistics for quantitative diffusion tensor MRI analysis.** *Med Image Comput Comput Assist Interv Int Conf Med Image Comput Comput Assist Interv* 2005;8:131–39
23. Corouge I, Fletcher PT, Joshi S, et al. **Fiber tract-oriented statistics for quantitative diffusion tensor MRI analysis.** *Med Image Anal* 2006;10:786–98
24. Looney CB, Smith JK, Fagan LH, et al. **Intracranial hemorrhage in asymptomatic neonates: prevalence on MR scans and relationship to obstetric and neonatal risk factors.** *Radiology* 2007;242:535–41
25. Mori S, Crain BJ, Chacko VP, et al. **Three-dimensional tracking of axonal projections in the brain by magnetic resonance imaging.** *Ann Neurol* 1999;45:265–69
26. Xu D, Mori S, Solaiyappan M, et al. **A framework for callosal fiber distribution analysis.** *Neuroimage* 2002;17:1131–43
27. Fillard P, Gilmore J, Lin W, et al. **Quantitative analysis of white matter fiber properties along geodesic paths.** *Lecture Notes Comp Scie* 2003;2879:16–23
28. Corouge I, Gouttard S, Gerig G. **A statistical shape model of individual fiber tracts extracted from diffusion tensor MRI.** *Medical Image Computing and Computer-Assisted Intervention—MICCAI 2004, Pt 2, Proceedings* 2004;3217:671–79
29. Goodlett C, Corouge I, Jomier M, et al. **A quantitative DTI fiber tract analysis suite.** *Insight J;* 2005 MICCAI Open-Source Workshop; Available at http://hdl.handle.net/1926/39, accessed August 20, 2007
30. Gerig G, Corouge I, Vachet C, et al. **Quantitative analysis of diffusion properties of white matter fiber tracts: A validation study.** International Society of Magnetic Resonance; Proceedings of ISMRM meeting May 7–13, 2005; Miami, Fla.; Page 1337
31. Yushkevich PA, Piven J, Hazlett HC, et al. **User-guided 3D active contour segmentation of anatomical structures: significantly improved efficiency and reliability.** *Neuroimage* 2006;31:1116–28
32. Kramer MS, Feinstein AR. **Clinical biostatistics. LIV. The biostatistics of concordance.** *Clin Pharmacol Ther* 1981;29:111–23
33. Rueckert D, Frangi AF, Schnabel JA. **Automatic construction of 3-D statistical deformation models of the brain using nonrigid registration.** *IEEE Trans Med Imaging* 2003;22:1014–25
34. Rueckert D, Hayes C, Studholme C, et al. **Non-rigid registration of breast MR images using mutual information.** *Medical Image Computing and Computer-Assisted Intervention—MICCAI'98* 1998;1496:1144–52
35. Wimberger DM, Roberts TP, Barkovich AJ, et al. **Identification of "premyelination" by diffusion-weighted MRI.** *J Comput Assist Tomogr* 1995;19:28–33
36. LaMantia AS, Rakic P. **Axon overproduction and elimination in the corpus callosum of the developing rhesus monkey.** *J Neurosci* 1990;10:2156–75
37. Beaulieu C. **The basis of anisotropic water diffusion in the nervous system—a technical review.** *NMR Biomed* 2002;15:435–55
38. Prayer D, Roberts T, Barkovich AJ, et al. **Diffusion-weighted MRI of myelination in the rat brain following treatment with gonadal hormones.** *Neuroradiology* 1997;39:320–25
39. Drobyshevsky A, Song SK, Gamkrelidze G, et al. **Developmental changes in diffusion anisotropy coincide with immature oligodendrocyte progression and maturation of compound action potential.** *J Neurosci* 2005;25:5988–97

The next 4 chapters discuss the various pathologic conditions of the mandible and maxilla; these include congenital, infectious, and neoplastic lesions. Plain radiographic and CT and MR features of several different conditions in each category of diseases are discussed to familiarize their imaging characteristics to both dental and other medical specialists. Although I appreciate that this work is not intended to be a textbook, it would have been helpful to include the clinical management of the various disease conditions as well as the cancer staging nomenclature of the different head and neck neoplasms and their treatment options.

The chapter related to the temporomandibular joint gives valuable practical information about the potential usefulness of state-of-the-art MR compared with previous conventional imaging modalities in practically all categories of diseases. In selected cases, illustrations from surgical and autopsy specimens that supplement the MR images are also very informative. The next 4 chapters elucidate the gamut of pathologic conditions that pertain to regions closely related to the jaw. These conditions include dental implants, maxillofacial trauma, craniofacial deformities, and disorders of the paranasal sinuses. The chapter on dental pathology, including implants, is a very useful overview for the medical profession because this area is well known to dentists. The potential of CT, including advanced conebeam techniques along with high-quality reconstructed images, is provided.

A comprehensive overview of the various types of maxillofacial fractures and imaging modalities, including advanced CT reconstruction modalities available in the different subtypes of fractures, is discussed at length in the chapter on facial trauma. In the chapter on disturbances of facial growth, a thorough review and illustrations of craniofacial anomalies, with emphasis on the complementary role of both 2D and 3D CT imaging, are discussed.

The next 2 chapters focus on the evolving role and advantages of advanced imaging techniques, namely CT and MR, compared with traditional dental/conventional plain radiographs (that dentists are more familiar with) in the diagnosis of diseases of the paranasal sinuses and the adjacent maxillofacial soft tissues, which include lesions of the oropharynx or oral cavity and deep neck spaces.

At the end of the book, a particularly useful chapter deals with lesions of the surrounding tissues that the radiologist will commonly encounter during the work-up of a patient with a maxillofacial lesion. Clinical and imaging characteristics of a potpourri of congenital, degenerative, inflammatory, infectious, and neoplastic conditions are discussed.

Finally, the last chapter includes various interventional procedures for the treatment of assorted pathologic conditions of the orbitofacial region that the maxillofacial radiologist may be asked to perform. Indications and techniques of procedures such as arthroscopy of the temporomandibular joint, a sialogram, biopsy of the deep neck space, and embolization of a hemangioma are briefly covered.

In summary, the authors have achieved their goal of providing an introduction to the role of advanced imaging modalities, primarily CT and MR, in maxillofacial imaging. Overall, this book is well organized and has a unique format that meets its intended purpose. It is a concise "atlas" that is simple to use and to the point, with a plethora of high-quality, clearly labeled illustrations. However, for particular topics in which specific details are needed, the audience should be warned that it may need to research other material as well. The authors are encouraged to use this book as a foundation for future editions of a more formal textbook on maxillofacial imaging. I recommend this book to anyone who is interested in maxillofacial radiology.

DOI 10.3174/ajnr.A0721

BOOK BRIEFLY NOTED

Cranial Nerves: Functional Anatomy

S. Monkhouse, ed. Cambridge, UK: Cambridge University Press; 2005,162 pages, $50.00.

This 162-page pocketbook, derived from notes made initially for Professor Monkhouse's medical students, would be useful both as a quick reference and as a good introduction to the cranial nerves. It is well organized; the first section is on the major concepts and basic anatomy of the cranial nerves and the subsequent 4 sections are organized by function. For example, all cranial nerves dealing with eye movement and sight are grouped together. Each chapter within a section introduces the pertinent cranial nerve or division, its basic anatomy, clinical-pathologic correlations and finally how the function of this nerve is tested in a clinical setting. There are 26 line drawings and 9 tables that help elucidate many of the concepts from the text.

DOI 10.3174/ajnr.A0832

BOOKS RECEIVED

Imaging of Head and Neck Cancer. A. Ahuja, R.M. Evans, A.D. King, C.A. van Hasselt, eds. London: Greenwich Medical Media Ltd.; 2003, $90.00.

Magnetic Resonance Imaging in Stroke. S. Davis, M. Fisher, S. Warach, eds. Cambridge, UK: Cambridge University Press; 2003, 280 pages, 21 line diagrams, 76 halftones, 14 color plates, 16 tables, $175.00.

Intervening in the Brain—Changing Psyche and Society Series: Ethics of Science and Technology Assessment, Vol. 2. R. Merkel, G. Boer, J. Fegert, T. Galert, D. Hartmann, B. Nuttin, S. Rosahl, eds. New York: Springer; 2007, 533 pages, 11 illustrations, $99.00.

Tumors of the Brain and Spine Series: M.D. Anderson Cancer Care Series. F. DeMonte, M.R. Gilbert, A. Mahajan, I.E. McCutcheon, eds. New York: Springer; 2007, 364 pages, 87 illustrations, $89.95.

Patch-Clamp Analysis: Advanced Techniques, 2nd ed. W. Walz, ed. Totowa, NJ: Humana Press; 2007, 424 pages, $125.00.

Radiobiological Modelling in Radiation Oncology. R. Dale, B. Jones, eds. London: British Institute of Radiology; 2007, 292 pages, $120.00.

Erratum

Please note that October article "Early Postnatal Development of Corpus Callosum and Corticospinal White Matter Assessed with Quantitative Tractography" by Gilmore et al (2007;28:1789–95) printed with incorrect DOI number 10.3174/ajnr.A0651. The correct DOI number is 10.3174/ajnr.A0751. This error has been corrected for the on-line version of the article.

DOI 10.3174/ajnr.A0868